

Neutron Spectroscopic Study of Anisotropic Exchange in the Dimer Compound $\text{Cs}_3\text{Ho}_2\text{Br}_9$

A. Furrer

*Labor für Neutronenstreuung, Eidgenössische Technische Hochschule Zürich,
c/o Paul Scherrer Institut, CH-5232 Villigen PSI, Switzerland*

H. U. Güdel and E. R. Krausz^(a)

Institut für Anorganische Chemie, Universität Bern, CH-3000 Bern 9, Switzerland

H. Blank

Institut Laue-Langevin, 156 X, F-38042 Grenoble CEDEX, France

(Received 10 July 1989)

The inelastic-neutron-scattering technique was used to measure magnetic excitations of Ho^{3+} dimers in $\text{Cs}_3\text{Ho}_2\text{Br}_9$. The usual phenomenological models failed to reproduce the observed energy spectra. An exchange-tensor formalism, on the other hand, which treats the Ho^{3+} ground state as an effective $S=2$ state, provides an excellent description of the observed energy splittings and intensities.

PACS numbers: 71.70.Gm, 75.20.Ck, 75.30.Et

Information on the nature of the coupling between magnetic spins has been slowly developing since the discovery of exchange by Heisenberg,¹ Dirac,² and Van Vleck³ (HDVV). For cases of well isolated orbital singlets the applicability of an isotropic HDVV Hamiltonian $J\mathbf{S}_1 \cdot \mathbf{S}_2$ has been amply confirmed by experiment. In cases of orbital degeneracy terms of the form $\mathbf{S}_1 \cdot \mathbf{A} \cdot \mathbf{S}_2$ have often been used to take account of the exchange anisotropy.

The elucidation of the exact nature of exchange in insulating rare-earth ion systems is complicated by a dearth of experimental data. We have shown that the study of dimer systems by inelastic neutron scattering (INS) provides a very direct way to establish exchange splittings and thus exchange parameters.⁴⁻⁶ Exchange anisotropy is expected to be particularly pronounced in rare-earth systems. It came as a surprise, therefore, that the exchange splittings observed by INS in the ground state of $\text{Cs}_3\text{Yb}_2\text{Br}_9$ and in the first excited crystalline-electric-field (CEF) state of $\text{Cs}_3\text{Tb}_2\text{Br}_9$ could be described by a HDVV Hamiltonian.^{5,6} In the meantime we have performed INS experiments on $\text{Cs}_3\text{Ho}_2\text{Br}_9$ involving the three lowest CEF states. We find it impossible to reproduce all the observed splittings by the usual phenomenological models,^{4,5} and we adopt a formalism using an exchange tensor $J(M_1, M_2; M'_1, M'_2)$ in which M_1, M_2 and M'_1, M'_2 represent the initial and final dimer states, respectively.^{7,8} However, for f electrons the number of independent parameters needed to describe the exchange tensor is very large,⁹ even after reduction by symmetry arguments. Approximations must be made to reduce this number. This can be achieved, e.g., by projecting the exchange interaction onto a basis defined by an effective total angular momentum \mathbf{S} of low dimension, the most familiar example being the replacement of an orbital doublet by an effective $S=\frac{1}{2}$ system. In the

present work we describe this procedure for the case of Ho^{3+} intradimer interactions in the compound $\text{Cs}_3\text{Ho}_2\text{Br}_9$. The energy spectra observed by the INS technique are sufficiently detailed to allow an analysis in terms of an exchange tensor in an effective $S=2$ model and thereby to arrive at a physically realistic description of exchange anisotropy in a rare-earth system. To our knowledge it has not been possible so far to ascertain from experiments individual elements of the exchange tensor $J(M_1, M_2; M'_1, M'_2)$. The apparent HDVV-like exchange in $\text{Cs}_3\text{Yb}_2\text{Br}_9$ and $\text{Cs}_2\text{Tb}_2\text{Br}_9$ is shown to be due to the fact that exchange splittings in only one CEF state were investigated.

$\text{Cs}_3\text{Ho}_2\text{Br}_9$ crystallizes in space group $R\bar{3}c$.¹⁰ The $\text{Ho}_2\text{Br}_9^{3-}$ dimers consist of two face-sharing HoBr_6^{3-} octahedra; they have D_3 (approximate D_{3h}) point symmetry, and their threefold axis coincides with the crystal c axis. We neglect interdimer interactions and write the spin Hamiltonian of a Ho^{3+} dimer as follows:

$$H = H_{\text{CEF}}(1) + H_{\text{CEF}}(2) + H_{\text{ex}}(1, 2), \quad (1)$$

where the first two terms are the usual single-ion Hamiltonians for a trigonal crystalline electric field (CEF).⁴ In the octahedral HoBr_6^{3-} environment the CEF operator splits the ground-state multiplet 5I_8 of Ho^{3+} with a total angular momentum $S=8$ into a Γ_3 ground state followed by a Γ_4 triplet and a Γ_1 singlet at 1 and 4 meV, respectively;¹¹ the remaining CEF states are above 15 meV. The trigonal symmetry C_3 (approximate C_{3v}) of Ho^{3+} in $\text{Cs}_3\text{Ho}_2\text{Br}_9$ further splits the cubic Γ_4 triplet into a Γ_1 singlet and a Γ_3 doublet.

The exchange operator $H_{\text{ex}}(1, 2)$ will further split the CEF states. As we may anticipate anisotropic exchange, we write phenomenologically

$$H_{\text{ex}}(1, 2) = -2J[r\mathbf{S}_1 \cdot \mathbf{S}_2 + (1 - |r|)S_1^z S_2^z]. \quad (2)$$

In this notation we have the Heisenberg model for $r = \pm 1$, the Ising model for $r=0$, and the xy model for $r = -0.5$. The effect of $H_{ex}(1,2)$ on the three lowest CEF states is illustrated in Fig. 1 for the antiferromagnetic exchange that usually occurs in these compounds.⁵ The symmetry designation of the dimer states is in D_{3h} . Details of the calculations are described in Ref. 5. Since we are only interested in the low-energy excitations, there is no need to consider more than the three lowest CEF states which altogether have a fivefold multiplicity. Calculations based on an effective $S=2$ model gave a very similar exchange splitting pattern and identical selection rules, which means that a truncation of the basis states, i.e., neglect of components with $M > 2$, is well justified.

The INS experiments were performed on the time-of-flight spectrometer IN5 at the high-flux reactor of the Institut Laue-Langevin in Grenoble. The wavelength of the incoming neutrons was varied between 4.8 and 8.0 Å, and the scattering angles covered the range from 2° to 134°. The samples were sealed in platelike aluminum containers of dimensions 45×40×4 mm³ and mounted in a helium cryostat ($T \geq 1.8$ K). The resulting time-of-flight spectra were corrected for transmission, detector efficiency, resolution effects, and sample-container scattering according to standard procedures. The polycrystalline compound $Cs_3Ho_2Br_9$ and its diluted analog $Cs_3Ho_{0.2}Y_{1.8}Br_9$ were synthesized as described in the literature.¹²

Experiments on the isostructural diluted compound $Cs_3Ho_{0.2}Y_{1.8}Br_9$ were used to determine the CEF splittings of single Ho^{3+} ions in this crystal environment. Figure 2 shows the results at low-energy transfers. We clearly identify two well resolved inelastic lines at 0.49 and 1.16 meV which we interpret as $\Gamma_3 \rightarrow \Gamma_1$ and $\Gamma_3 \rightarrow \Gamma_3$ transitions (C_{3v} notation), respectively. In the

energy spectra observed for the undiluted compound $Cs_3Ho_2Br_9$ (top of Fig. 2) the effect of exchange coupling manifests itself in an enhanced width and some fine structure of the inelastic lines. This is particularly pronounced for the peak at around 0.5 meV which is composed of at least three individual lines. The intensity distribution is strongly dependent upon the modulus of the scattering vector Q as revealed by the measurements with increased resolution shown in Fig. 3. With increasing Q we observe a transfer of intensity from the central component to the two outer lines; in addition, an unresolved shoulder starts to show up on the low-energy side. This Q dependence of the intensities is an important means to identify particular transitions within the exchange-splitting pattern as outlined in detail in Ref. 5.

We have made fits to the high-resolution energy spectra with four Gaussians, using a least-squares procedure. The results are shown by the solid and broken curves in Fig. 3. Using the temperature dependence in addition to the Q dependence it was possible to unambiguously assign the four lines to particular transitions and thus to derive the energy splitting pattern shown in Fig. 4. Our interpretation is confirmed by the rather nice agreement between the observed and calculated intensities displayed in Fig. 4. The level sequence, however, is incompatible with any exchange-splitting pattern resulting from the anisotropic exchange Hamiltonian (2); see Fig. 1. Firstly, Eq. (2) neither yields Γ_2 as the ground state (except in combination with Γ_1), nor places Γ_6 in between Γ_1 and Γ_2 (except for unrealistically high values of J). Secondly, our experiments indicate a similar range of exchange splittings for the three lowest CEF states (see Figs. 2 and

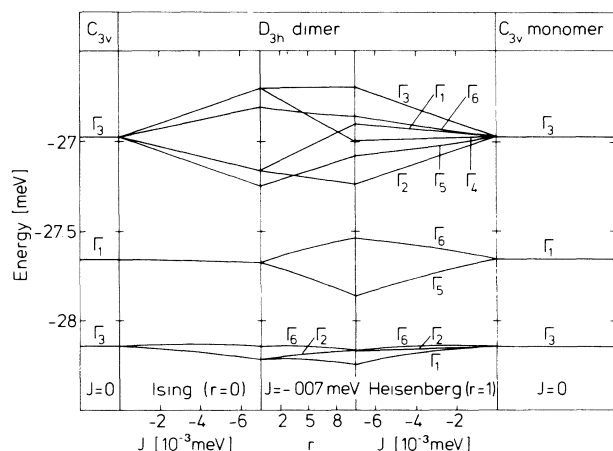


FIG. 1. Exchange-induced splitting of the three lowest CEF states of a Ho^{3+} dimer for antiferromagnetic exchange defined by Eq. (2) using the full CEF level scheme ($S=8$ for Ho^{3+}).

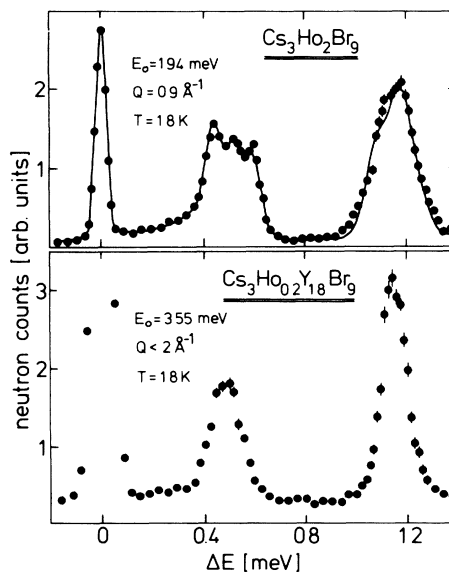


FIG. 2. Energy spectra of neutrons scattered for polycrystalline $Cs_3Ho_2Br_9$ and $Cs_3Ho_{0.2}Y_{1.8}Br_9$. The curve corresponds to the calculated energy spectrum based on the model parameters of Eq. (6).

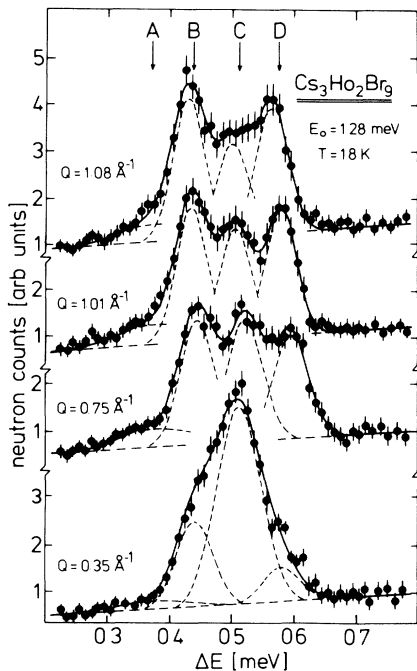


FIG. 3. Energy spectra of neutrons scattered from polycrystalline $\text{Cs}_3\text{Ho}_2\text{Br}_9$. The curves are explained in the text.

4), which cannot be realized by Eq. (2). In particular, the calculated exchange splitting of the excited Γ_3 CEF state typically exceeds that of the Γ_3 ground state by a factor of 7 (see Fig. 1). The failure of the widely used phenomenological model is evident, and our highly informative INS data clearly require a different approach.

We adopt the exchange tensor formalism⁷⁻⁹ and treat our $\Gamma_3, \Gamma_1, \Gamma_3$ CEF manifold as an effective $S=2$ state. The interaction Hamiltonian thus takes the form

$$H_{\text{ex}}(1,2) = -2J(M_1, M_2; M'_1, M'_2) \mathbf{S}_1 \cdot \mathbf{S}_2, \quad (3)$$

which involves a 25×25 exchange tensor. Symmetry relations drastically reduce the number of independent exchange parameters; for a pair of identical ions we have

$$\begin{aligned} J(M_1, M_2; M'_1, M'_2) &= J(M_2, M_1; M'_2, M'_1) \\ &= J(-M_1, -M_2; -M'_1, -M'_2) \\ &= J(M'_1, M'_2; M_1, M_2), \end{aligned} \quad (4)$$

and the axial symmetry requires⁷

$$(M_1 - M'_1) + (M_2 - M'_2) = 0. \quad (5)$$

Equations (4) and (5) limit the number of independent nonvanishing exchange parameters to 22; restriction to bilinear exchange further reduces this number to fifteen. We have examined in detail the exchange splittings induced by each of the fifteen bilinear exchange parameters. The following results evolve from these considerations: Firstly, only the parameter $J(1,0;0,1)$ is able to

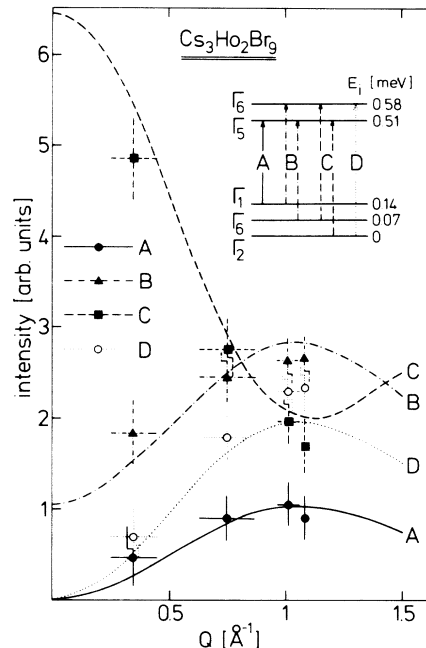


FIG. 4. Q dependence of the intensities of the low-energy exchange splittings displayed in Fig. 3. The lines denote the calculated values. Inset: The resulting low-energy level sequence.

appreciably split the excited Γ_1 CEF state. Secondly, only the parameters $J(2,1;1,2)$ and $J(2,-2;1,-1)$ are able to realize the observed ground-state level sequence $\Gamma_2-\Gamma_6-\Gamma_1$ (see Fig. 4); in addition, the parameter $J(2,1;1,2)$ produces by far the biggest splitting of the excited Γ_3 CEF state. Thirdly, the remaining parameters have little influence on the exchange splitting and compensate each other to a large extent. As a consequence we are able to describe the observed energy spectra with only three parameters, namely

$$\begin{aligned} J(1,0;0,1) &= -7 \times 10^{-3} \text{ meV}, \\ J(2,1;1,2) &= -2 \times 10^{-2} \text{ meV}, \\ J(2,-2;1,-1) &= 6 \times 10^{-2} \text{ meV}, \end{aligned} \quad (6)$$

which excellently reproduce the observed exchange splittings of both the CEF ground state Γ_3 and the excited state Γ_1 to within 0.01 meV. The available spectral information on the exchange-split CEF excited state Γ_3 is not sufficiently detailed to allow a rigorous check of the model parameters. However, as shown in Fig. 2, the overall exchange splitting is in very good agreement with experiment. This is particularly gratifying, because the upper Γ_3 exchange splitting was calculated to be too large by almost an order of magnitude in the model equation (2).

In conclusion, our high-resolution neutron spectroscopic data on the exchange splitting of Ho^{3+} dimers in $\text{Cs}_3\text{Ho}_2\text{Br}_9$ provide a stringent test for theoretical mod-

els. Our analysis in terms of an exchange tensor formalism [Eq. (3)] and an effective $S=2$ state is superior to the phenomenological Hamiltonian Eq. (2). It was thus possible to directly determine, for the first time, the leading components of the exchange tensor $J(M_1, M_2; M'_1, M'_2)$ and to establish the anisotropy of the spin coupling in a rather detailed manner. There are ferromagnetic as well as antiferromagnetic exchange tensor elements [see Eq. (6)], and the nature of the spin coupling is purely transverse, i.e., $\Delta M = \pm 1$. This is in contrast to recent findings obtained for $\text{Cs}_3\text{Yb}_2\text{Br}_9$ and $\text{Cs}_2\text{Tb}_2\text{Br}_9$ where the observed exchange splittings could be interpreted with a simple isotropic antiferromagnetic Hamiltonian.^{5,6} Calculations show, however, that the experimental results can be equally well reproduced by the exchange tensor formalism. A rigorous discrimination between the HDVV and the tensor model is not possible because of the insufficient number of observed transitions. In particular, the INS measurements performed for $\text{Cs}_3\text{Yb}_2\text{Br}_9$ and $\text{Cs}_3\text{Tb}_2\text{Br}_9$ only gave information on the exchange splitting of a single CEF state, whereas the present data on $\text{Cs}_3\text{Ho}_2\text{Br}_9$ elucidating the exchange splittings of three CEF states are much more comprehensive and detailed. We therefore feel that the apparent HDVV-like exchange interaction derived for $\text{Cs}_3\text{Yb}_2\text{Br}_9$ and $\text{Cs}_3\text{Tb}_2\text{Br}_9$ (and possibly for many other f -electron compounds) is related to the limited information supplied by

the experiments.

Financial support by the Swiss National Science Foundation is gratefully acknowledged.

^(a)Present address: Research School of Chemistry, Australian National University, Canberra, Australian Capital Territory 2601, Australia.

¹W. Heisenberg, *Z. Phys.* **38**, 411 (1986).

²P. A. M. Dirac, *Proc. Roy. Soc. London A* **112**, 661 (1926).

³J. H. Van Vleck, in *The Theory of Electric and Magnetic Susceptibilities* (Cambridge Univ. Press, Oxford, 1932).

⁴A. Furrer, H. U. Güdel, and J. Darriet, *J. Less-Common Met.* **111**, 223 (1985).

⁵A. Furrer, H. U. Güdel, H. Blank, and A. Heidemann, *Phys. Rev. Lett.* **62**, 210 (1989).

⁶A. Dönni, A. Furrer, H. Blank, A. Heidemann, and H. U. Güdel, *J. Phys. (Paris), Colloq.* **49**, C8-1513 (1988).

⁷P. M. Levy, in *Magnetic Oxides, Part 1*, edited by D. J. Craik (Wiley, New York, 1975), p. 181.

⁸W. P. Wolf, *J. Phys. (Paris), Colloq.* **32**, C1-26 (1971).

⁹P. M. Levy, *Phys. Rev.* **177**, 509 (1969).

¹⁰G. Meyer, *Z. Anorg. Allg. Chem.* **445**, 140 (1978).

¹¹A. Furrer, H. U. Güdel, and N. Furer, Eidgenössische Technische Hochschule Zürich Report No. LNS-137, 1987 (unpublished), p. 75.

¹²G. Meyer, *Inorg. Synth.* **22**, 1 (1983).